

Macrophage-Myofibroblast Transition as a Potential Origin for Skeletal Muscle Fibrosis After Injury via Complement System Activation

Beijie Qi^{1,*}, Yuqi Li^{2,*}, Zhen Peng², Zhiwen Luo³, Xingyu Zhang², Jiwu Chen², Guoqi Li², Yaying Sun²

¹Department of Orthopedics, Shanghai Pudong Hospital, Fudan University Pudong Medical Center, Shanghai, People's Republic of China; ²Department of Sports Medicine, Shanghai General Hospital, Shanghai Jiao Tong University School of Medicine, Shanghai Jiao Tong University, Shanghai, People's Republic of China; ³Department of Sports Medicine, Huashan Hospital, Fudan University, Shanghai, People's Republic of China

*These authors contributed equally to this work

Correspondence: Yaying Sun; Guoqi Li, Tel +86 17621642602; +86 13816307547, Email yaying.sun@shgh.cn; etherlords@163.com

Background: Acute skeletal muscle injury is common in sports. The injured muscle cannot fully recover due to fibrosis resulting from myofibroblasts. Understanding the origin of fibroblasts is, therefore, important for the development of anti-fibrotic therapies. Accumulating evidence shows that a mechanism called macrophage-myofibroblast transition (MMT) can lead to tissue or organ fibrosis, yet it is still unclear whether MMT exists in skeletal muscle and the exact mechanisms.

Methods: Single-cell transcriptome of mice skeletal muscle after acute injury was analyzed with a specific attention on the process of MMT. Cell-cell interaction network, pseudotime trajectory analysis, Gene Ontology (GO), and Kyoto Genome Encyclopedia (KEGG) were conducted. A series of experiments in vivo and in vitro were launched for verification.

Results: Single cell transcriptomic analysis indicated that, following acute injury, there were much interactions between macrophages and myofibroblasts. A detailed analysis on macrophages indicated that, CD68⁺α-SMA⁺ cells, which represented the status of MMT, mainly appeared at five days post-injury. KEGG/GO analysis underlined the involvement of complement system, within which C3ar1, C1qa, C1qb, and C1qc were up-regulated. Trajectory analysis also confirmed a potential shift from macrophages to myofibroblasts. These findings were verified by histological study in mice skeletal muscle, that there were much MMT cells at five days, declined gradually, and vanished 14 days after trauma, when there was remarkable fibrosis formation within the injured muscle. Moreover, C3a stimulation could directly induce MMT in BMDMs.

Conclusion: Fibrosis following acute injury is disastrous to skeletal muscle, but the origin of myofibroblasts remains unclear. We proved that, following acute injury, macrophage-myofibroblast transition happened in skeletal muscle, which may contribute to fibrosis formation. This phenomenon mainly occurred at five days post-injury. The complement system can activate MMT. More evidence is needed to directly support the pro-fibrotic role of MMT in skeletal muscle fibrosis after acute injury.

Keywords: skeletal muscle, fibrosis, macrophage-myofibroblast transition, single-cell transcriptomic analysis, complement system

Introduction

Acute skeletal muscle injury is prevalent in sports which can be caused by contusion, laceration, or strain. The incidence of skeletal muscle injury varies from 10% to 55%.¹ Immediately after injury, skeletal muscle initiates healing process, promoting myofiber regeneration and extracellular matrix (ECM) re-construction.² Newly-formed ECM provides good basis for myoblasts proliferation, fusion³ and myofiber growth,⁴ and re-organizes gradually.⁵ However, in some cases, the injured skeletal muscle may not fully recover due to the formation of fibrosis tissue, which is caused by excessive ECM production. Fibrosis tissue impairs regeneration and contraction of skeletal muscle, and further increases re-injury rate.⁶ Therefore, treatments against fibrosis are critical to the healing of skeletal muscle.

The progress of acute skeletal muscle fibrosis is related to exorbitant local inflammation and fibrogenic differentiation of myoblasts.⁷ During the early inflammatory phase, monocytes are activated and differentiate to M1 macrophages. The pro-inflammatory M1 macrophages are then recruited to clear injured muscle fibers and stimulate the proliferation of myoblasts.⁸ Once the necrotic fiber debris are removed, M1 macrophages are subsequently polarized into M2 macrophages, secreting anti-inflammatory factors and induce myoblast differentiation and myotube formation.⁸ Fibroblasts also differentiate into myofibroblasts during this period, leading to skeletal muscle fibrosis.⁹

The origin of myofibroblasts is a subject of intense debate. Resident fibroblasts,¹⁰ myoblasts,¹¹ and even perivascular cells¹² can all serve as the pool of myofibroblasts after acute skeletal muscle injury. In recent years, accumulating evidence suggests a new cellular origin of myofibroblasts called macrophage-to-myofibroblast transition (MMT). Studies indicated that monocyte/macrophages from bone marrow can transform into myofibroblasts in a mouse model of unilateral ureteric obstruction.¹³ Wang also found MMT phenomenon which contributes to interstitial fibrosis in human chronic active renal allograft injury as identified by co-expression of macrophage (CD68 or F4/80) and myofibroblast (α -SMA) markers.¹⁴ Little et al demonstrated MMT in the subretinal fibrotic lesion which led to subretinal fibrosis.¹⁵ These observations indicate that MMT might be another pathway causing myofibroblast accumulation during fibrosis disease. However, it remains unknown whether MMT occurs in skeletal muscle and the exact mechanisms.

Recent years have witnessed the wide application of single-cell sequencing for studying biological systems with unparalleled resolution and improved our understanding of cell-type composition, differentiation dynamics, rare cell types, transcriptome response under external signals in many diseases, including tissue fibrosis.¹⁶ Yang utilized single-cell transcriptomic analysis to reveal a transcriptional roadmap for the activation of HSCs during liver fibrosis,¹⁷ and Havermann demonstrated the profibrotic role of distinct epithelial and mesenchymal lineages in pulmonary fibrosis with single-cell RNA sequencing.¹⁸ On ground of this, we first analyzed the single-cell transcriptome of mice skeletal muscle after acute injury with a specific attention on the process of MMT, and then conducted a series of experiments in vitro and in vivo to confirm the findings in silico, in an attempt to providing potential targets against skeletal muscle fibrosis after acute injury.

Methods

Data Download

Two single-cell transcriptomic datasets (GSE143437 and GSE138826) of skeletal muscle sample from wild-type C57 mice were retrieved from Gene Expression Omnibus (<https://www.ncbi.nlm.nih.gov/geo/>) database. The tibialis anterior (TA) of each mouse was injured via intramuscular injection of cardiotoxin. Both TA muscles per time-point/per mouse received injection while the counterpart was non-injured. Three time points were selected for analysis, ie, 5 days post-injury (D5, n=6), 2 days post-injury (D2, n=5), and non-injured control (D0, n=6).

Single-cell RNA Sequencing Data Processing

Conducted by R (version 4.2.2), the data were first converted to Seurat objects using the Seurat (v4.4.0) and then filtered according to the following requirements: (i) the number of genes detected in a single cell >500 and <8000; (ii) the percentage of mitochondrial genes detected in a single cell <5%. Gene expression matrices were generated by log normalization and linear regression using the NormalizeData and ScaleData functions in the Seurat. Principal component analysis was performed using the RunPCA function for dimensional reduction clustering. DecontX was applied to predict contamination level when mixing datasets to remove aberrant expression of marker genes. Sample-level batch effects were eliminated by Applied Harmony. Cell subpopulations were visualized by TSNE and UMAP, and characteristic gene expression was visualized using Seurat software (Dotplot, FeaturePlot, and other functions). Differential expression analysis was achieved via Seurat's "FindAllMarkers" function using a likelihood ratio test which assumes the data follows a negative binomial distribution, and only considering genes with > log₂(0.25) fold-change in >25% of cells within the cluster. Cell types were identified using "Single R" software, reports from published researches,¹⁹ and experience.

Cell–Cell Interaction Network Analysis

Based on the gene expression level, potential cellular ligand–receptor interactions between the subpopulation of immunocytes were determined by CellPhoneDB. Pairs with $P < 0.05$ were considered statistically significant. Cell types were assigned to particular ligands and receptors to exhibit the cell–cell interaction network. “CellChat” R package (version 1.6.1) was applied to infer the intercellular communication.

Identification of Macrophages Subtypes and Cell Developmental Trajectory Analysis

Macrophages in single-cell data were extracted and the process of dimensional reduction and clustering was repeated using Seurat software. We then used the Seurat “FindAllClusters” to find differentially expressed genes that characterize the subpopulations. The R package Slingshot v1.410 was used to perform pseudotime trajectory analysis in macrophages independently. The expression of fibrogenic markers, including Col1a1, Fn1, and Vim, as well as the membrane receptor of C3a (C3ar1) were also examined across different cell types.

Analysis of GO and KEGG Functions

The level of Acta2 gene expression divided macrophages of D5 into two groups. The “quickMarkers” function in SoupX package was used to compare the Acta2+ and Acta2- groups with a criteria of P value < 0.05 . The Metascape database (www.metascape.org) was used for annotation and visualization, and the differential genes were analyzed by Gene Ontology (GO) and Kyoto Genome Encyclopedia (KEGG)²⁰ pathway analysis to obtain the biological functions and signaling pathways involved. Enrichment was deemed statistically significant when the overlap was ≥ 3 with $P \leq 0.01$.

Animal Feeding and Model Establishment

Animal experiments were performed according to the Guide for the Care and Use of Laboratory Animals and the experimental protocol was approved by the local committee. Thirty C57/6J mice of ~10 weeks old were subject to contusion injury on the left tibialis anterior (TA) under anesthetization as aforementioned.²¹ Animals were allowed to move freely after trauma. At 1, 3, 5, 7, and 14 days post-injury (group D1, D3, D5, D7, and D14, respectively), 6 random mice were sacrificed for harvesting the injured TA ($n=6$). Another three mice of the same batch served as the un-injured control (group D0) and were sacrificed for bilateral TA collection at the time when the group D14 were sacrificed.

Histological Measurements

Intact or injured TA samples were dissected and frozen in OCT with liquid nitrogen precooled and stored at -80°C for sectioning. Samples were cut into 8- μm thickness for routine HE, Masson staining, as well as immunofluorescence staining for proteins of interest by the established protocol.²² The quantification of relative fluorescence of CD68, α -SMA, F4/80, and Col 1 took D0 as reference, while that of the co-expression of CD68 plus α -SMA (or F4/80 plus Col1) took D5 as reference. Primary antibodies used were anti-F4/80 (ab300421), anti- α -SMA (ab7817), anti-CD68 (ab125212), and anti-Col 1 (sc-293182). DAPI (blue) located nuclei. Images were observed by fluorescence microscope (ECHO Revolve, America).

Cell Culture and Stimulation

Bone marrow-derived macrophages (BMDMs) were prepared following an established protocol.²³ Bone marrow cells were flushed out from tibia, femur, and ilium bone. The bone marrow cells were differentiated for one week in DMEM/F12 with 10% FBS and 50 ng/mL recombinant mouse macrophage colony-stimulating factor (Gibco). Purity of BMDMs was validated by immunofluorescent staining of F4/80. For C3a (novoprotein, No.: CM99) stimulation, 10 ng/mL recombinant mouse C3a¹⁵ was added into the medium for 72h and then collected for measurements.

Western Blot Analysis

Cells were lysed by RIPA (Beyotime Biotechnology, Haimen, China) with protease and phosphatase inhibitor cocktail (Pierce, Thermo Fisher Scientific), centrifuged, and heated. The protein expression was analyzed by Western blot as

previously described.²⁴ Anti- α -SMA (ab7817), anti-Col 1 (ab270993), and Tubulin (AF7011) were used. Bands were captured by Bio-Rad ChemiDocXRS+ and relative band intensity was obtained via normalization to Tubulin (n=3).

Immunofluorescent Staining

Immunofluorescence staining on BMDMs was conducted as described elsewhere.²² Primary antibodies used were anti-F4/80 (ab6640) and anti-Col 1 (ab270993). DAPI was used to locate nuclei. Images were observed by fluorescence microscopy with ImageJ software for quantification. The expression was obtained from six random high-power fields and divided by cell count (DAPI), and normalized to the value of group NC.

Statistical Analysis

Presented as mean \pm SD, data was analyzed in GraphPad Prism 7.0 (GraphPad Software, La Jolla, USA). Significance was analyzed by Student's *t*-test or one-way ANOVA followed by post hoc Tukey test, $P < 0.05$ was regarded as statistically significant.

Results

Cell-Type and Gene-Expression Dynamics of Acute Muscle Injury at Single-Cell Resolution

The sequential alteration in cell components and gene expression following muscle injury is shown in Figure 1. Overall, we discerned 10 distinct cell populations via SNN clustering (Figure 1A). Within the uninjured muscles (Day 0) there were mainly endothelial cells, fibro/adipogenic progenitors (FAPs), and stromal cells, with other cell populations, especially immune cells, were detected infrequently. However, following injury, multiple immune cell types (ie, macrophages, neutrophils and T cells) increased remarkably at D2 and/or D5 (Figure 1B).

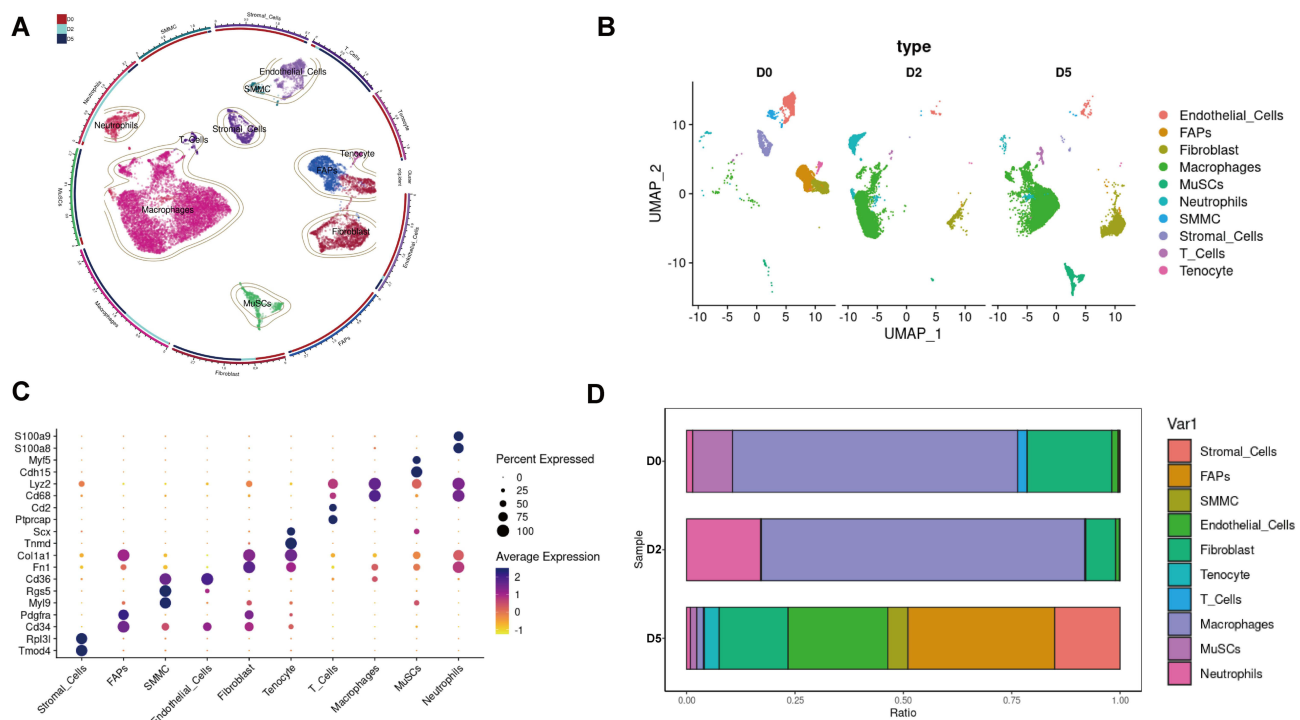


Figure 1 Single cell transcriptome analysis of mice skeletal muscle after acute injury. **(A)** UMAP embedding of scRNA-seq data colored by meta-clusters to simplify visualization. **(B)** UMAP embedding of scRNA-seq data colored by meta-clusters and split by time point to visualization. **(C)** Dot plots grouped by meta-clusters demonstrate cell-type marker gene expression, which was used to classify metaclusters. Identification of cell types from SNN clusters based on cluster-average expression of canonical genes. Dot size represents the percentage of cells with a non-zero expression level and color-scale represents the average expression level across all cells within cluster. **(D)** Relative proportion of cell types at each time point.

Representative markers of each cell subpopulation is listed in Figure 1C. As a substantial player for skeletal muscle homeostasis,²⁵ Pdgfra⁺ FAPs occupied about 30% of the mononuclear cell population at D0 (~30%), followed by Cdh5-expressing endothelial cells ranked second at D0 (25%).²⁶ Contrarily, muscle satellite cells (MuSCs) expressed Pax7 and Myf5 were trace population in D0 or D2, and exploded at D5, indicating an extremely active status in the repair. Immune cell populations also exhibited notable dynamics within this atlas. At D0, the proportion of immune cell populations is minute and can be subdivided into more defined groups of S100a9⁺ S100a8⁺ neutrophils, Cd3g⁺ T cells, and a set of macrophages expressing Lyz2, Cd68. The number of neutrophils increase in D2, subsequently decreasing in D5, reflecting an acute inflammation reaction after injury. Moreover, macrophages increased sharply from D0 to D2 and D5 (Figure 1D).

Cell-cell chat analysis deciphered the ligand-receptor reactions among different cell types (Figure 2A). Vigorous crosstalk between immune cells and interstitial cells, especially that between macrophages and fibroblasts (Figure 2B), were described, suggesting a strong immune-repair interaction early after acute injury.

Dynamic Analysis of Macrophages After Acute Injury

Macrophages are a major regulator of tissue regeneration following trauma.²⁷ We therefore extracted all macrophages for dimensional reduction and clustering. Unsupervised SNN clustering resolved 5 distinct subpopulations belonging to pro-

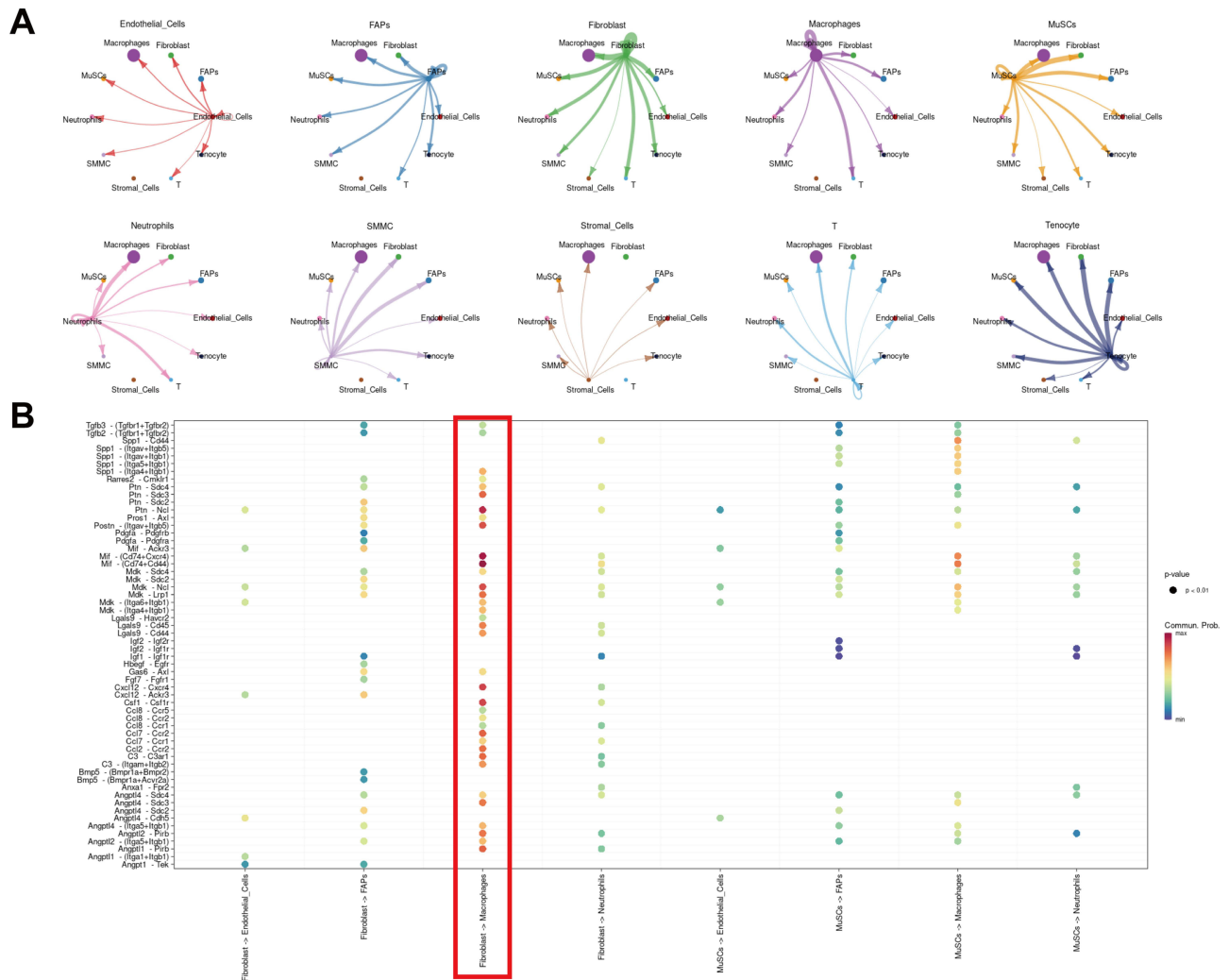


Figure 2 Major interactions between key cells in injured skeletal muscle. (A) netVisual_circle to demonstrate number of interaction in any two cell types. (B) Dot plot of all ligand-receptor results in the specified receptor ligand cell type. Red box illustrates the crosstalk between fibroblasts and macrophages.

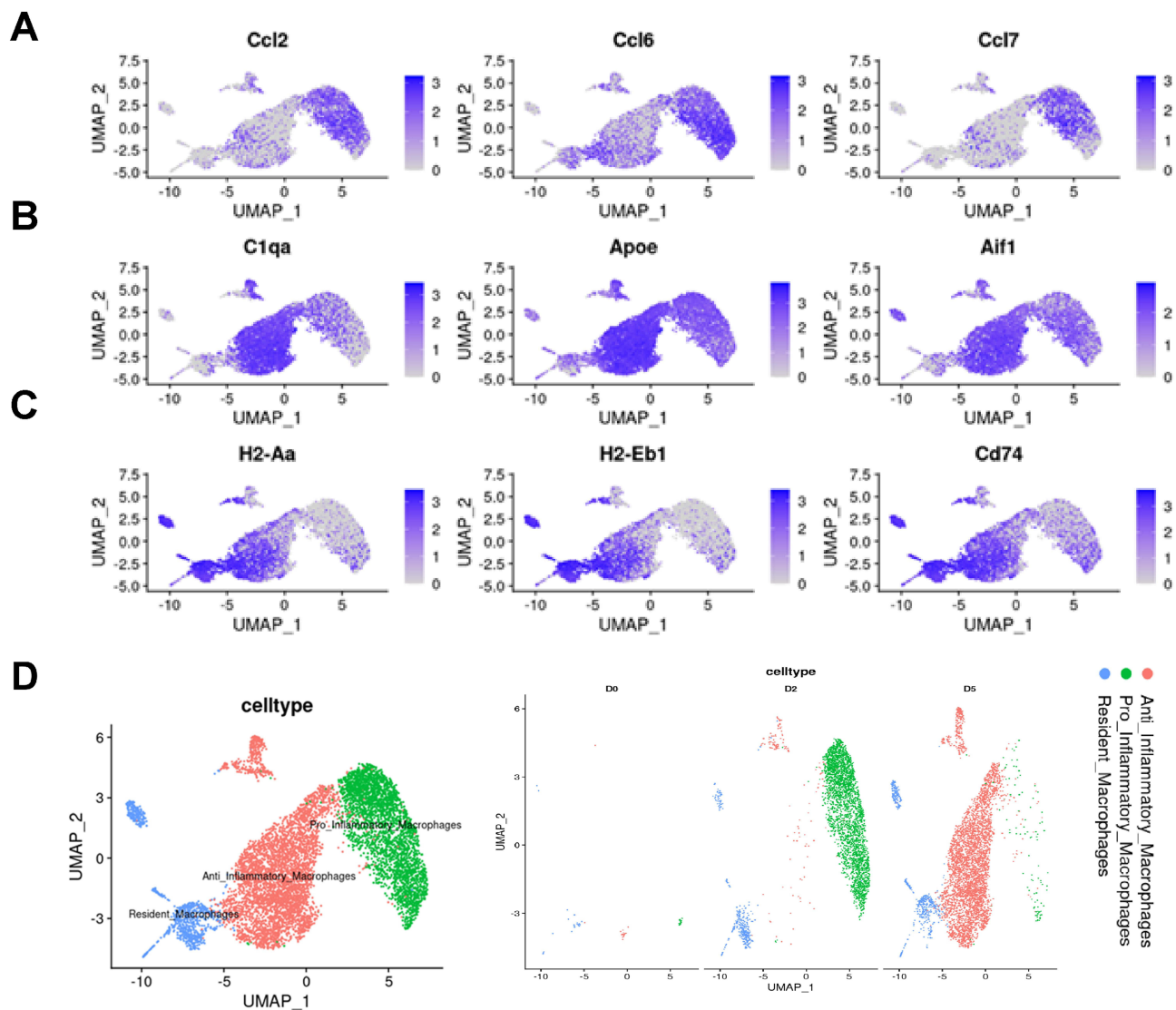


Figure 3 Single cell transcriptome analysis of macrophages. (A) Single-cell expression levels for selecting pro-Inflammatory macrophages gene markers. (B) Single-cell expression levels for select anti-Inflammatory macrophages gene markers. (C) Single-cell expression levels for select resident macrophages gene markers. (D) (left) UMAP atlas of macrophages single-cell transcriptomes. Cells colored by subsets of macrophages. (right) UMAP embedding of macrophages colored by subsets and split by time point to visualization.

inflammatory (Figure 3A), anti-inflammatory macrophages (Figure 3B), and resident macrophages (Figure 3C) according to established markers.¹² UMAP of macrophages split by time point displayed conspicuous dynamics. At D2, macrophages were mainly composed of pro-inflammatory macrophages, while this phenotype shifted dramatically into anti-inflammatory macrophages at D5 (Figure 3D).

To better understand the transition of macrophages along the timeline, we inferred pseudotime trajectories by slingshot. The pseudotime trajectory presented an organized progression of cells from pro-inflammatory macrophages, the leading phenotype in D2, to cycling and committed progenitors to anti-inflammatory macrophages, the primary phenotype in D5 (Figure S1).

Macrophage-Myofibroblast Transition Occurred in the Injured Skeletal Muscle

Moreover, we noticed a cluster of CD68⁺α-SMA⁺ macrophages (Figure 4A) by FeaturePlot, the key event of MMT.²⁸ In detail, this cell subtype predominantly expressed in anti-inflammatory macrophages at D5 (Figure 4B). By dividing the anti-inflammatory macrophages at D5 into Acta2⁺ and Acta2⁻ cells, we compared the differentially expressed genes

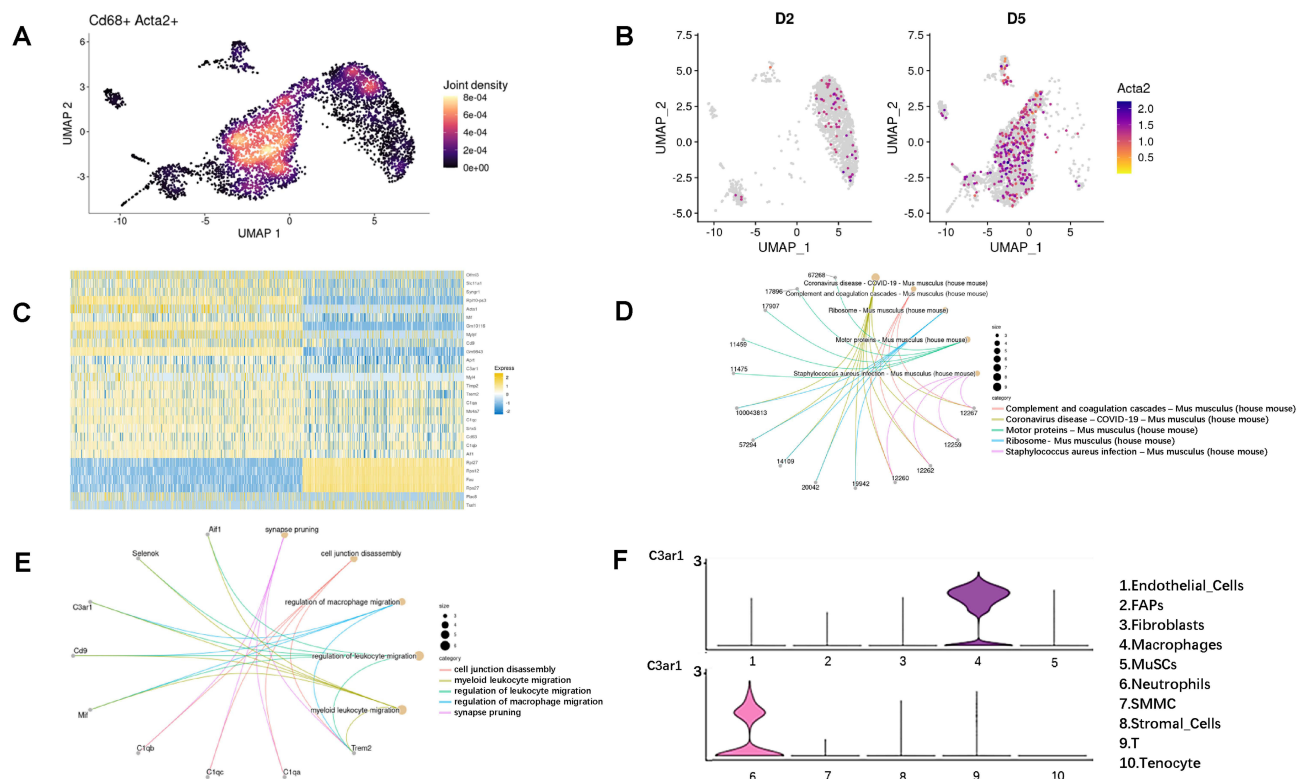


Figure 4 Detailed analysis of Cd68+Acta2+ cells undergoing MMT. (A) Plot_Density_Joint_Only to demonstrate distribution of CD68+Acta2+ cell in macrophages. (B) Plot_Density_Joint_Only to demonstrate expression of Acta2 genes in macrophages post acute injury. (C) Heatmap generated by comparison of Acta2+ cells and Acta2- cells in D5 (D5 post-injury) to evaluate transcriptional characteristics differentially expressed across two groups. (D and E) KEGG and GO analysis, respectively. (F) ViolinPlot to demonstrate expression of C3ar1 level in all cell types.

(Figure 4C) with KEGG (Figure S2) and GO (Figure S3) analysis. Some genes participated in more than one pathway (Figure 4D and E).

Interestingly, we found complement and coagulation cascades network was activated in Acta2⁺ anti-inflammatory macrophages. Genes involved in this pathway, ie, C3ar1, C1qa, C1qb and C1qc, were all up-regulated (Table S1) and were predominantly expressed in macrophages (Figure 4F), especially the anti-inflammatory macrophages (Figure S4). Monocell pseudotime trajectory uncovered the relationship between macrophages and myofibroblasts, illustrating a start from macrophages towards myofibroblasts where MMT cells located along the trajectory without obvious spatial bias (Figure S5).

The above findings in silico were verified in vivo. After confirming the model establishment via HE and Masson staining which showed infiltrated inflammatory cells, newborn myofibers, and collagen deposition in a sequential manner (Figure 5A), immunofluorescence staining was conducted to analyze the expression of macrophages and myofibroblasts in skeletal muscle after contusion. As shown in Figure 5B, the expression of CD68 gradually up-regulated from D0 to D5 and declined at D7 and D14, while that of α -SMA increased in a timely sequence (Figure 5C and D). Importantly, we noticed a group of cells positive of CD68 and α -SMA which mounted at D5, the direct evidence of the presence of MMT, which took a significant portion of α -SMA+ cells and CD68+ cells respectively in D5 and D7 (Figure 5E and F). The same effect was also seen in the immunofluorescence staining of the expression of F4/80 and Col 1 (Figure S6). Similarly, the expression of C3ar1 peaked at D5 and D7 (Figure S7).

C3a Was Enough to Trigger Macrophage-Myofibroblast Transition in BMDMs

To further verify the above findings, the fibrogenic characteristics of different cells involved in the regulation of ECM, including fibroblasts and MuSCs, were depicted bioinformatically. Interestingly, either macrophages, fibroblasts, or

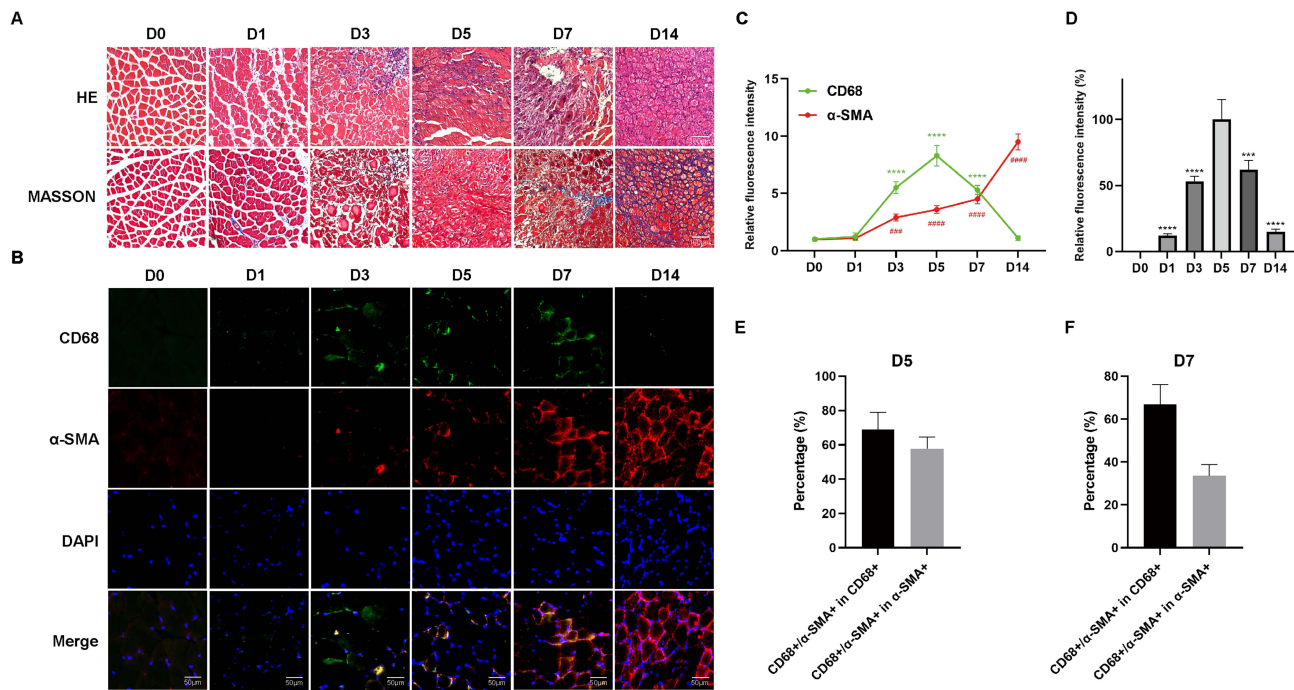


Figure 5 The macrophage-myofibroblast transition process in skeletal muscle after contusion. **(A)** HE staining was utilized to demonstrate the inflammatory infiltration and newborn muscle fibers, while MASSON staining showed the collagen deposition in the healing process of skeletal muscle after contusion. **(B)** The representative immunofluorescence images demonstrated the location and relative expression of CD68 and α -SMA. **(C)** Quantification of relative fluorescence intensity of CD68 and α -SMA respectively. (n=6) Data was presented as mean \pm SD. *** p <0.0001, #### p <0.001, and ##### p <0.0001 compared to the value of D0. **(D)** Quantification of relative fluorescence intensity of co-expression of CD68 and α -SMA. (n=6) Data was presented as mean \pm SD. ** p <0.001 and **** p <0.0001 compared to the value of D5. **(E)** Quantification of percentage of co-expression of CD68 with α -SMA in CD68+ or α -SMA at D5. (n=6) Data was presented as mean \pm SD. **(F)** Quantification of percentage of co-expression of CD68 with α -SMA in CD68+ or α -SMA at D7. (n=6) Data was presented as mean \pm SD.

MuSCs have positive expression of fibrogenic markers Coll1a1, Fn1, and Vim (Figure S8A), but only macrophages have the expression of C3ar1 (Figure S8B), so we next examined the effect of C3a on BMDMs.

After a successful cell harvest (Figure 6A), we stimulated the cells with C3a. Fluorescent imaging noticed significant up-regulation of Col 1 in BMDMs (Figure 6B and quantified in C), WB also indicated an elevated expression of α -SMA and Col 1 in BMDMs after C3a stimulation (Figure 6D and quantified in E and F). Together, these findings validated the appearance of MMT following acute skeletal muscle injury, which could be a result of complement challenge.

Discussion

Fibrosis formation following acute skeletal muscle injury is a troublesome issue, and myofibroblasts play a key role in this pathological process. In the current study, by integrative analysis of single-cell data as well as experiments in vitro and in vivo, we noticed a novel origin of myofibroblasts, ie, myofibroblasts originated from macrophages, also known as MMT.²⁸ Moreover, we noticed that complement and related pathways were activated during MMT and C3a was enough to trigger MMT in BMDMs.

Skeletal muscle is composed of multinucleated myofibers and a pool of MuSCs, FAPs, endothelial cells, and resident immune cells.²⁹ Upon acute injury, both MuSCs and FAPs are activated, proliferate, differentiate, or even secrete various factors for the repair of injury. Meanwhile, this process is finely regulated by an ordered immune response, such as the early infiltration of neutrophils, subsequent polarization of macrophages.³⁰ For macrophages, M1 phenotype appears early in the injured site to initiate inflammation response and clear necrotic tissue, and then transfers into M2 phenotype to support tissue repair by secreting growth factors.^{31,32} In line with the established knowledge above, we noticed that, pro-inflammatory macrophages were mainly detected at D2, while at D5, anti-inflammatory macrophages were mainly detected.

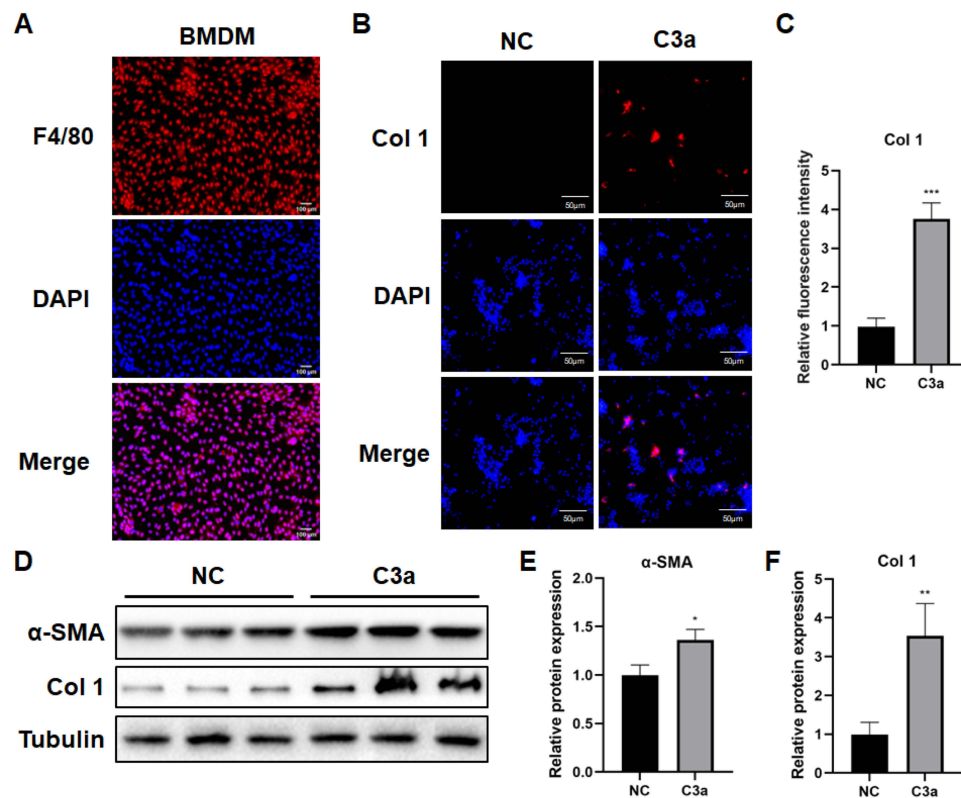


Figure 6 MMT was induced in BMDMs with the stimulation of C3a. (A) The representative immunofluorescence image demonstrated the location and relative expression of F4/80. Scale bar = 100 μ m. (B) The representative immunofluorescence image demonstrated the relative expression of Col 1. Scale bar = 50 μ m. (C) Quantification of relative fluorescence intensity of Col 1. (n=6) ***p<0.001. (D) α -SMA and Col 1 expression level was determined by Western blot after different treatment. (E and F) Quantification of relative protein expression. (n=6) Data was presented as mean \pm SD. *p<0.05, **p<0.01.

A coordinated transition from M1 to M2 macrophages is essential for skeletal muscle repair, otherwise injured skeletal muscle will have vast scar formation and collagen deposition.³³ However, what happened to macrophages next? This concern was still unclear. Previous studies suggested that macrophages experience apoptosis finally.^{34,35} On the contrary, in recent years, Lan reported a group of evidence that macrophages differentiate into myofibroblasts to exacerbate fibrotic process via various mechanisms in renal fibrosis.^{36–38} Similar phenomenon were subsequently noticed in proliferative vitreoretinal disorder,³⁹ bladder fibrosis,⁴⁰ and lung fibrosis.⁴¹ In agreement with these findings, we also noticed an apparent MMT process within the early period following skeletal muscle contusion.

Acute skeletal muscle injury is commonly seen in sports and traumas. In this research, manifested by HE and Masson staining, we found increasingly inflammatory cell infiltration early after contusion, newborn muscle fibers, and a continuously accumulated collagen deposition, validating an acute injury model establishment. During the post-trauma period, macrophages continuously increased from D1 to D5 and then decreased, verifying a participation early after acute injury. On the other hand, myofibroblasts, marked by α -SMA and Col 1, was elevating gradually, which reflected the fibrotic process. Importantly, MMT was captured within the injured site via co-expression of CD68 plus α -SMA or F4/80 plus Col 1 from D3 to D7, mounting at D5. These observations, no doubt, indicated a possible participation of MMT in skeletal muscle recovery after trauma, especially the fibrogenic process.

To further solidify the above findings, we conducted a series of experiments on BMDMs, the exact cell experiencing MMT.^{37,38} We found that, C3a significantly enhanced the expression of fibrogenic capability of BMDMs. Apart from infection and inflammation-related disorder, C3a receptor signaling broadly participates tissue and organ regeneration.^{42,43} In skeletal muscle, C3ar1, C1qa, C1qb, and C1qc were all significantly up-regulated at D2 following skeletal muscle injury, while interfering with C3a-C3ar1 signaling at this timepoint significantly inhibited macrophage recruitment and the subsequent regeneration process.⁴⁴ On the other hand, we proved that the up-regulation of C3ar1,

C1qa, C1qb, and C1qc remained significantly up-regulated in MMT cells, indicating a dual role of complement signaling pathway, especially C3a-C3ar1 pathway, in skeletal muscle repair. That is, the prolonged activation of this signaling pathway would be harmful than beneficial, since this would drive macrophages into myofibroblasts, eventually leading to fibrosis. To solidify this speculation, we tested the effect of C3a on BMDMs, the pivotal player during MMT.^{37,38} Not surprisingly, C3a significantly enhanced the expression of fibrogenesis-related markers, including α -SMA and Col 1.

How C3a stimulates the MMT process of macrophages is not fully understood. Little et al verified that C3a triggers MMT, but the detailed mechanisms are not deeply explored.¹⁵ Based on established evidence, downstream of C3ar1 includes PLC, STAT3, Ras/c-Raf, and GSK β , et al, with various functions in different cell types.⁴⁵ Since complement is an important player of the immune system, direct intervention may increase the risk of immune disturbance.⁴⁶ Therefore, there is a need to unveil the key factor mediating the pro-MMT function of C3a on macrophages, so as to reach deeper understanding of skeletal muscle repair.

The current research is a valuable foundation for future researches in skeletal muscle biology. Most importantly, although we have confirmed MMT phenomenon in skeletal muscle injury model, and verified that this progress was under the stimulation of C3a, whether MMT is merely a negative event resulting in fibrosis formation or it is also a required process for skeletal muscle healing should be investigated directly so as to provide therapeutic directions. Besides, MMT is observed in the acute muscle injury model, does this phenomenon also exist in aging-related muscle regeneration, and what is the exact significance of this phenomenon needs to be clarified. Additionally, since the complement system is required for skeletal muscle regeneration, the exact time to manipulate the complement system in the injured site for the promotion other than inhibition of skeletal muscle regeneration should be explored. When delivering anti-complement drugs, one should bear the risk of major side effects such as an increased risk of infection, aberrant cell regeneration and metabolism, as well as suppressed clearance of immune complexes.⁴⁶ Therefore, detailed changes within BMDMs after C3a stimulation should be delineated for the purpose of precision medicine.

Our finding should also be interpreted with caution. First, the results we obtained were dependent on mice single-cell transcriptome and mice BMDMs, the phenotype changes of human BMDMs and different macrophage cell lines, such as Raw264.7 and THP-1, should also be detected to warrant the current findings. Second, in the analysis *in silico*, the two datasets used different agents, ie, notexin and cardiotoxin respectively, to induce skeletal muscle injury. Both chemicals are commonly used venoms for inducing skeletal muscle injury and regeneration, and comparisons between the two have been published previously showing that both mycotoxins could result in an overall destruction of skeletal muscle with similar inflammatory cytokine changes, but the influence on regeneration is largely dependent on dosage and batch.⁴⁷ This information suggested heterogeneity between two agents. On the other hand, this concern was partially addressed by our bioinformatics analysis that the overall and acta2+ macrophages had similar distribution. Besides, in our study design, contusion was applied as this is a model with clinical relevance. Still, there is a difference between contusion and venom-induced skeletal muscle injury, and more investigations were needed to illustrate if there was a difference between contusion-induced and venom-induced MMT process. Finally, whether MMT process directly contributes to skeletal muscle fibrosis following contusion is not proven. Based on the expression of membrane receptor of C3a across different cell populations, further experiments focusing on the relationship between C3ar1 blockade at 3–5 days post injury and skeletal muscle fibrosis should be conducted to make the current inference robust.

Conclusion

Skeletal muscle fibrosis following acute injury is unavoidable and disastrous, but the origin of myofibroblasts remains to be uncovered. For the first time, we proved that, following acute injury, macrophage-myofibroblast transition happened in skeletal muscle in response to complement C3a challenge, and is a source of collagen formation. Whether this process plays a role in the fibrosis formation of skeletal muscle following trauma needs further investigations with direct evidence. In addition, studies are required to decipher the detailed changes within macrophages, with an attempt to treat skeletal muscle fibrosis or facilitate regeneration.

Ethics Approval

This study was approved by the ethics committee of by the Animal Care Committee of Fudan University. All experiments related to animals were conducted abiding by the National Institutes of Health Guide for the Care and Use of Laboratory Animals.

Acknowledgments

Thanks for the help of Dr. Huiyao Lan, who first identified and reported the MMT phenomenon, from The Chinese University of Hong Kong-Guangdong Academy of Sciences/Guangdong Provincial People's Hospital Joint Research Laboratory on Immunological and Genetic Kidney Diseases, The Chinese University of Hong Kong, Hong Kong, China for his kind help on properties of BMDMs in experiment design.

Funding

This work was supported by the National Natural Science Foundation of China (No. 82102634, No. 81972062, No. 82172509).

Disclosure

The authors declare that they have no competing interests in this work.

References

1. Beiner JM, Jokl P. Muscle contusion injuries: current treatment options. *J Am Acad Orthop Surg.* 2001;9(4):227–237. doi:10.5435/00124635-200107000-00002
2. Gardner T, Kenter K, Li Y. Fibrosis following acute skeletal muscle injury: mitigation and reversal potential in the clinic. *J Sports Med.* 2020;2020:7059057. doi:10.1155/2020/7059057
3. Liu X, Gao Y, Long X, et al. Type I collagen promotes the migration and myogenic differentiation of C2C12 myoblasts via the release of interleukin-6 mediated by FAK/NF- κ B p65 activation. *Food Funct.* 2020;11(1):328–338. doi:10.1039/C9FO01346F
4. Delaney K, Kasprzycka P, Ciemerych MA, et al. The role of TGF- β 1 during skeletal muscle regeneration. *Cell Biol Int.* 2017;41(7):706–715. doi:10.1002/cbin.10725
5. Alameddine HS, Morgan JE. Matrix metalloproteinases and tissue inhibitor of metalloproteinases in inflammation and fibrosis of skeletal muscles. *J Neuromusc Dis.* 2016;3(4):455–473. doi:10.3233/JND-160183
6. Mahdy MAA. Skeletal muscle fibrosis: an overview. *Cell Tissue Res.* 2019;375(3):575–588. doi:10.1007/s00441-018-2955-2
7. Nozaki M, Li Y, Zhu J, et al. Improved muscle healing after contusion injury by the inhibitory effect of suramin on myostatin, a negative regulator of muscle growth. *Am J Sports Med.* 2008;36(12):2354–2362. doi:10.1177/0363546508322886
8. Wang Y, Lu J, Liu Y. Skeletal muscle regeneration in cardiotoxin-induced muscle injury models. *Int J Mol Sci.* 2022;23(21):13380.
9. Jung M, Ma Y, Iyer RP, et al. IL-10 improves cardiac remodeling after myocardial infarction by stimulating M2 macrophage polarization and fibroblast activation. *Basic Res Cardiol.* 2017;112(3):33. doi:10.1007/s00395-017-0622-5
10. Gibb AA, Huynh AT, Gaspar RB, et al. Glutamine uptake and catabolism is required for myofibroblast formation and persistence. *J Mol Cell Cardiol.* 2022;172:78–89. doi:10.1016/j.yjmcc.2022.08.002
11. Sun Y, Wang H, Li Y, et al. miR-24 and miR-122 negatively regulate the transforming growth factor-beta/smad signaling pathway in skeletal muscle fibrosis. *Mol Ther Nucleic Acids.* 2018;11:528–537. doi:10.1016/j.omtn.2018.04.005
12. Dulauroy S, Di Carlo SE, Langa F, et al. Lineage tracing and genetic ablation of ADAM12(+) perivascular cells identify a major source of profibrotic cells during acute tissue injury. *Nat Med.* 2012;18(8):1262–1270. doi:10.1038/nm.2848
13. Wang S, Meng X-M, Ng -Y-Y, et al. TGF-beta/Smad3 signalling regulates the transition of bone marrow-derived macrophages into myofibroblasts during tissue fibrosis. *Oncotarget.* 2016;7(8):8809–8822. doi:10.18632/oncotarget.6604
14. Wang YY, Jiang H, Pan J, et al. Macrophage-to-myofibroblast transition contributes to interstitial fibrosis in chronic renal allograft injury. *J Am Soc Nephrol.* 2017;28(7):2053–2067. doi:10.1681/ASN.2016050573
15. Little K, Llorián-Salvador M, Tang M, et al. Macrophage to myofibroblast transition contributes to subretinal fibrosis secondary to neovascular age-related macular degeneration. *J Neuroinflammation.* 2020;17(1):355. doi:10.1186/s12974-020-02033-7
16. Grun D, van Oudenaarden A. Design and analysis of single-cell sequencing experiments. *Cell.* 2015;163(4):799–810. doi:10.1016/j.cell.2015.10.039
17. Yang W, He H, Wang T, et al. Single-cell transcriptomic analysis reveals a hepatic stellate cell-activation roadmap and myofibroblast origin during liver fibrosis in mice. *Hepatology.* 2021;74(5):2774–2790. doi:10.1002/hep.31987
18. Habermann AC, Gutierrez AJ, Bui LT, et al. Single-cell RNA sequencing reveals profibrotic roles of distinct epithelial and mesenchymal lineages in pulmonary fibrosis. *Sci Adv.* 2020;6(28):eaba1972. doi:10.1126/sciadv.aba1972
19. Aran D, Looney AP, Liu L, et al. Reference-based analysis of lung single-cell sequencing reveals a transitional profibrotic macrophage. *Nat Immunol.* 2019;20(2):163–172. doi:10.1038/s41590-018-0276-y
20. Sun Y, Sun X, Liu S, et al. The overlap between regeneration and fibrosis in injured skeletal muscle is regulated by phosphatidylinositol 3-kinase/Akt signaling pathway - A bioinformatic analysis based on lncRNA microarray. *Gene.* 2018;672:79–87. doi:10.1016/j.gene.2018.06.001

21. Luo Z, Lin J, Sun Y, et al. Bone marrow stromal cell-derived exosomes promote muscle healing following contusion through macrophage polarization. *Stem Cells Dev.* 2021;30(3):135–148. doi:10.1089/scd.2020.0167
22. Sun Y, Chen W, Hao Y, et al. Stem cell-conditioned medium promotes graft remodeling of midsubstance and intratunnel incorporation after anterior cruciate ligament reconstruction in a rat model. *Am J Sports Med.* 2019;47(10):2327–2337. doi:10.1177/0363546519859324
23. Tang PC, Chung JY-F, Xue VW-W, et al. Smad3 promotes cancer-associated fibroblasts generation via macrophage-myofibroblast transition. *Adv Sci.* 2022;9(1):e2101235. doi:10.1002/advs.202101235
24. Sun Y, Luo Z, Chen Y, et al. si-Tgfb1-loading liposomes inhibit shoulder capsule fibrosis via mimicking the protective function of exosomes from patients with adhesive capsulitis. *Biomater Res.* 2022;26(1):39. doi:10.1186/s40824-022-00286-2
25. De Micheli AJ, Laurillard EJ, Heinke CL, et al. Single-cell analysis of the muscle stem cell hierarchy identifies heterotypic communication signals involved in skeletal muscle regeneration. *Cell Rep.* 2020;30(10):3583–3595 e5. doi:10.1016/j.celrep.2020.02.067
26. Giordani L, He GJ, Negroni E, et al. High-dimensional single-cell cartography reveals novel skeletal muscle-resident cell populations. *Mol Cell.* 2019;74(3):609–621 e6. doi:10.1016/j.molcel.2019.02.026
27. Wynn TA, Vannella KM. Macrophages in tissue repair, regeneration, and fibrosis. *Immunity.* 2016;44(3):450–462. doi:10.1016/j.immuni.2016.02.015
28. Tang PM, Nikolic-Paterson DJ, Lan HY. Macrophages: versatile players in renal inflammation and fibrosis. *Nat Rev Nephrol.* 2019;15(3):144–158. doi:10.1038/s41581-019-0110-2
29. Paylor B, Natarajan A, Zhang RH, Rossi F. Nonmyogenic cells in skeletal muscle regeneration. *Curr Top Dev Biol.* 2011;96:139–165.
30. Tidball JG, Villalta SA. Regulatory interactions between muscle and the immune system during muscle regeneration. *Am J Physiol Regul Integr Comp Physiol.* 2010;298(5):R1173–87. doi:10.1152/ajpregu.00735.2009
31. Moyer AL, Wagner KR. Regeneration versus fibrosis in skeletal muscle. *Curr Opin Rheumatol.* 2011;23(6):568–573. doi:10.1097/BOR.0b013e32834bac92
32. Serhan CN, Savill J. Resolution of inflammation: the beginning programs the end. *Nat Immunol.* 2005;6(12):1191–1197. doi:10.1038/ni1276
33. Luo Z, Qi B, Sun Y, et al. Engineering bioactive M2 macrophage-polarized, anti-inflammatory, miRNA-based liposomes for functional muscle repair: from exosomal mechanisms to biomaterials. *Small.* 2022;18(34):e2201957. doi:10.1002/sml.202201957
34. Yang X, Chang Y, Wei W. Emerging role of targeting macrophages in rheumatoid arthritis: focus on polarization, metabolism and apoptosis. *Cell Prolif.* 2020;53(7):e12854. doi:10.1111/cpr.12854
35. Yang G, Yang Y, Liu Y, et al. Regulation of alveolar macrophage death in pulmonary fibrosis: a review. *Apoptosis.* 2023;28(11–12):1505–1519. doi:10.1007/s10495-023-01888-4
36. Meng X-M, Wang S, Huang X-R, et al. Inflammatory macrophages can transdifferentiate into myofibroblasts during renal fibrosis. *Cell Death Dis.* 2016;7(12):e2495. doi:10.1038/cddis.2016.402
37. Tang PM, Zhang -Y-Y, Xiao J, et al. Neural transcription factor Pou4f1 promotes renal fibrosis via macrophage-myofibroblast transition. *Proc Natl Acad Sci U S A.* 2020;117(34):20741–20752. doi:10.1073/pnas.1917663117
38. Tang PM, Zhou S, Li CJ, et al. The proto-oncogene tyrosine protein kinase Src is essential for macrophage-myofibroblast transition during renal scarring. *Kidney Int.* 2018;93(1):173–187. doi:10.1016/j.kint.2017.07.026
39. Abu El-Asrar AM, De Hertogh G, Allegaert E, et al. Macrophage-myofibroblast transition contributes to myofibroblast formation in proliferative vitreoretinal disorders. *Int J Mol Sci.* 2023;24(17):13510. doi:10.3390/ijms241713510
40. Wang W, Xiao D, Lin L, et al. Antifibrotic effects of tetrahedral framework nucleic acids by inhibiting macrophage polarization and macrophage-myofibroblast transition in bladder remodeling. *Adv Healthc Mater.* 2023;12(11):e2203076. doi:10.1002/adhm.202203076
41. Yang F, Chang Y, Zhang C, et al. UUO induces lung fibrosis with macrophage-myofibroblast transition in rats. *Int Immunopharmacol.* 2021;93:107396. doi:10.1016/j.intimp.2021.107396
42. Marshall KM, He S, Zhong Z, et al. Dissecting the complement pathway in hepatic injury and regeneration with a novel protective strategy. *J Exp Med.* 2014;211(9):1793–1805. doi:10.1084/jem.20131902
43. Mastellos DC, Deangelis RA, Lambris JD. Complement-triggered pathways orchestrate regenerative responses throughout phylogeny. *Semin Immunol.* 2013;25(1):29–38. doi:10.1016/j.smim.2013.04.002
44. Zhang C, Wang C, Li Y, et al. Complement C3a signaling facilitates skeletal muscle regeneration by regulating monocyte function and trafficking. *Nat Commun.* 2017;8(1):2078. doi:10.1038/s41467-017-01526-z
45. Pekna M, Stokowska A, Pekny M. Targeting complement C3a receptor to improve outcome after ischemic brain injury. *Neurochem Res.* 2021;46(10):2626–2637. doi:10.1007/s11064-021-03419-6
46. Schafer N, Grassel S. Involvement of complement peptides C3a and C5a in osteoarthritis pathology. *Peptides.* 2022;154:170815. doi:10.1016/j.peptides.2022.170815
47. Hardy D, Besnard A, Latil M, et al. Comparative study of injury models for studying muscle regeneration in mice. *PLoS One.* 2016;11(1):e0147198. doi:10.1371/journal.pone.0147198